



ISSN 1001-0742
CN 11-2629/X

2012

Volume **24**
Number **5**

JOURNAL OF
**ENVIRONMENTAL
SCIENCES**



Sponsored by
Research Center for Eco-Environmental Sciences
Chinese Academy of Sciences

CONTENTS

Aquatic environment

- Immunotoxic potential of aeration lagoon effluents for the treatment of domestic and Hospital wastewaters in the freshwater mussel *Elliptio complanata*
Franc is Gagn , Chantale Andr , Marl ne Fortier, Michel Fournier 781
- Spatial distribution of archaeal and bacterial ammonia oxidizers in the littoral buffer zone of a nitrogen-rich lake
Yu Wang, Guibing Zhu, Lei Ye, Xiaojuan Feng, Huub J. M. Op den Camp, Chengqing Yin 790
- Accelerated biodegradation of nitrophenols in the rhizosphere of *Spirodela polyrrhiza*
Risky Ayu Kristanti, Masahiro Kanbe, Tadashi Toyama, Yasuhiro Tanaka, Yueqin Tang, Xiaolei Wu, Kazuhiro Mori 800
- Sorption of 2,4-dinitroanisole (DNAN) on lignin
Rabih Saad, Zorana Radovic-Hrapovic, Behzad Ahvazi, Sonia Thiboutot, Guy Ampleman, Jalal Hawari 808
- Sewage sludge disintegration by high-pressure homogenization: A sludge disintegration model
Yuxuan Zhang, Panyue Zhang, Boqiang Ma, Hao Wu, Sheng Zhang, Xin Xu 814
- Degradation kinetics and mechanism of aniline by heat-assisted persulfate oxidation
Xiaofang Xie, Yongqing Zhang, Weilin Huang, Shaobing Huang 821
- Degradation of some typical pharmaceuticals and personal care products with copper-plating iron doped Cu₂O under visible light irradiation
Jing An, Qixing Zhou 827
- Preparation of high concentration polyaluminum chloride by chemical synthesis-membrane distillation method with self-made hollow fiber membrane
Changwei Zhao, Yong Yan, Deyin Hou, Zhaokun Luan, Zhiping Jia 834
- Characteristics of gas-liquid pulsed discharge plasma reactor and dye decoloration efficiency
Bing Sun, Nyein Nyein Aye, Zhiying Gao, Dan Lv, Xiaomei Zhu, Masayuki Sato 840
- Photolysis kinetics and influencing factors of bisphenol S in aqueous solutions
Guiping Cao, Jilai Lu, Gongying Wang 846
- Comparative study of leaching of silver nanoparticles from fabric and effective effluent treatment
Aneesh Pasricha, Sant Lal Jangra, Nahar Singh, Neeraj Dilbaghi, K. N. Sood, Kanupriya Arora, Renu Pasricha 852

Atmospheric environment

- Size distribution and chemical composition of secondary organic aerosol formed from Cl-initiated oxidation of toluene
Mingqiang Huang, Weijun Zhang, Xuejun Gu, Changjin Hu, Weixiong Zhao, Zhenya Wang, Li Fang 860
- Real-world fuel efficiency and exhaust emissions of light-duty diesel vehicles and their correlation with road conditions
Jingnan Hu, Ye Wu, Zhishi Wang, Zhenhua Li, Yu Zhou, Haitao Wang, Xiaofeng Bao, Jiming Hao 865
- Operating condition influences on PCDD/Fs emissions from sinter pot tests with hot flue gas recycling
Yongmei Yu, Minghui Zheng, Xianwei Li, Xiaolei He 875
- Size distribution of chemical elements and their source apportionment in ambient coarse, fine, and ultrafine particles in Shanghai urban summer atmosphere
Senlin L , Rui Zhang, Zhenkun Yao, Fei Yi, Jingjing Ren, Minghong Wu, Man Feng, Qingyue Wang 882
- Synergistic effects of non-thermal plasma-discharge catalyst and ultrasound on toluene removal
Yongli Sun, Libo Zhou, Luhong Zhang, Hong Sui 891
- Absorption characteristics of new solvent based on a blend of AMP and 1,8-diamino-*p*-menthane for CO₂ absorption
Sang-Sup Lee, Seong-Man Mun, Won-Joon Choi, Byoung-Moo Min, Sang-Won Cho, Kwang-Joong Oh 897

Terrestrial environment

- Toxicity and subcellular distribution of cadmium in wheat as affected by dissolved organic acids
Dandan Li, Dongmei Zhou 903
- Changes in the sorption, desorption, distribution, and availability of copper, induced by application of sewage sludge on Chilean soils contaminated by mine tailings
Tatiana Garrido, Jorge Mendoza, Francisco Arriagada 912
- Mechanism of lead immobilization by oxalic acid-activated phosphate rocks
Guanjie Jiang, Yonghong Liu, Li Huang, Qingling Fu, Youjun Deng, Hongqing Hu 919
- Methyl- -cyclodextrin enhanced biodegradation of polycyclic aromatic hydrocarbons and associated microbial activity in contaminated soil
Mingming Sun, Yongming Luo, Peter Christie, Zhongjun Jia, Zhengao Li, Ying Teng 926
- Inhibitory effect of nitrobenzene on oxygen demand in lake sediments
Xiaohong Zhou, Xuying Wang, Hanchang Shi 934

Environmental health and toxicology

- Endogenous nitric oxide mediates alleviation of cadmium toxicity induced by calcium in rice seedlings
Long Zhang, Zhen Chen, Cheng Zhu 940
- Species-dependent effects of the phenolic herbicide ioxynil with potential thyroid hormone disrupting activity: modulation of its cellular uptake and activity by interaction with serum thyroid hormone-binding proteins
Sakura Akiyoshi, Gobun Sai, Kiyoshi Yamauchi 949

Environmental catalysis and materials

- A screen-printed, amperometric biosensor for the determination of organophosphorus pesticides in water samples
Junfeng Dou, Fuqiang Fan, Aizhong Ding, Lirong Cheng, Raju Sekar, Hongting Wang, Shuairan Li 956
- A GFP-based bacterial biosensor with chromosomally integrated sensing cassette for quantitative detection of Hg(II) in environment
Himanshu Priyadarshi, Absar Alam, Gireesh-Babu P, Rekha Das, Pankaj Kishore, Shivendra Kumar, Aparna Chaudhari 963

Absorption characteristics of new solvent based on a blend of AMP and 1,8-diamino-*p*-menthane for CO₂ absorption

Sang-Sup Lee¹, Seong-Man Mun², Won-Joon Choi³, Byoung-Moo Min⁴,
Sang-Won Cho⁵, Kwang-Joong Oh^{2,*}

1. Department of Environmental Engineering, Chungbuk National University, Cheongju 361-763, Korea

2. Department of Environmental Engineering, Pusan National University, Busan 609-735, Korea. E-mail: tlossm@pusan.ac.kr

3. Corporate R&D Institute, Fuel Cell System Development Team, Doosan Heavy Industries & Construction, Daejeon 305-811, Korea

4. Greenhouse Gas Research Center, Korea Institute of Energy Research, Daejeon 305-343, Korea

5. Department of Energy and Environment, Korea Polytechnic VII College, Gyeongnam 642-020, Korea

Received 28 April 2011; revised 05 October 2011; accepted 28 October 2011

Abstract

Aqueous 1,8-diamino-*p*-menthane (KIER-C3) and commercially available amine solutions were tested for CO₂ absorption. A 2-amino-2-methyl-1-propanol (AMP) solution with an addition of KIER-C3 showed 9.3% and 31.6% higher absorption rate for CO₂ than the AMP solution with an addition of monoethanolamine (MEA) and ammonia (NH₃), respectively. The reaction rate constant for CO₂ absorption by the AMP/KIER-C3 solution was determined by the following equation: $k_{2,AMP/C3} = 7.702 \times 10^6 \exp(-2248.03/T)$. A CO₂ loading ratio of the AMP/KIER-C3 solution was also 2 and 3.4-times higher than that of the AMP/NH₃ solution and the AMP/MEA solution, respectively. Based on the experimental results, KIER-C3 may be used as an excellent additive to increase CO₂ absorption capability of AMP.

Key words: carbon dioxide; absorption rate and capacity; 1,8-diamino-*p*-menthane; 2-amino-2-methyl-1-propanol

DOI: 10.1016/S1001-0742(11)60788-2

Introduction

Global warming has become one of the most complicated issues in the world. Carbon dioxide (CO₂) is recognized as a major greenhouse gas generated in large quantities from various emission sources including fossil-fuel electric power plants, synthetic ammonia industries, steel production works, etc. (Gadalla et al., 2005). Although a number of techniques have been tested for the separation of CO₂ from fossil fuel fired flue gas, an economically viable process is not currently available. Therefore, a more efficient CO₂ recovery process still needs to be developed.

Many studies have been conducted to develop more efficient alkanolamine absorbents for CO₂. A zwitterion mechanism was proposed for the CO₂ absorption mechanism of the alkanolamine absorbent by Caplow (1968) and Danckwerts (1979). Different from monoethanolamine (MEA), sterically hindered amines form unstable carbamates due to the bulkiness of the carbon groups attached to the amino group. The hydrolysis of carbamates then forms bicarbonate and restores the free amines which can react with additional carbon dioxide (Sartori and Savage, 1983). A representative sterically hindered amine, 2-amino-2-methyl-1-propanol (AMP) has therefore a higher CO₂

loading capacity than MEA (Dawodu and Meisen, 1994).

Using a single amine can cause relatively fast corrosion and degradation reactions (Choi et al., 2009). Hence more effective and consistent absorption for CO₂ is expected by using a blend of two or more amines (Hornig and Li, 2002). A number of studies related to the kinetics of CO₂ absorption into a blend of aqueous amine solutions containing AMP have been conducted (Lee et al., 2008; Aroonwilas and Veawab, 2004; Xu et al., 1991). The blended amine solutions containing showed significant enhancement in the absorption capacity and absorption rate for CO₂ maintaining the characteristics of sterically hindered amines (Li and Chang, 1994).

In this study, KIER-C3 was examined for its possibility as an additive to AMP for CO₂ absorption using a lab-scale reactor. Reactivity of KIER-C3 with CO₂ was evaluated comparing with other additives such as MEA and NH₃ in terms of CO₂ absorption rate, reaction kinetics and CO₂ loading. Its performance was also tested under various operating conditions.

1 Materials and methods

1.1 Materials

AMP, MEA, NH₃ and 1,8-diamino-*p*-menthane (KIER-

* Corresponding author. E-mail: kjoh@pusan.ac.kr

C3) were used in this study as CO₂ absorbents. We obtained 95% AMP and 70% KIER-C3 from Sigma Aldrich (USA), 99% MEA from Yakuri Pure Chemicals (Japan), and 30% NH₃ from Junsei Chemical (Japan). Each solution was diluted with distilled water to a certain concentration. The purity of CO₂, N₂ and N₂O gases in each cylinder was 99.9%.

1.2 Apparatus and procedure

A schematic diagram of the experimental set up is presented in Fig. 1. Absorption experiments were carried out using an agitated glass reactor with an internal diameter of 7.3 cm and a height of 15.1 cm. Each solution of 150 mL was located inside the reactor at 313 K and agitated at 50 r/min. N₂ and CO₂ gases were premixed in the mixing chamber and then injected into the solution. The flow rates of N₂ and CO₂ gases were controlled using mass flow controllers (5850E, Brooks Instruments, USA, accuracy: $\pm 1\%$ of full scale) to maintain the CO₂ concentration of 15%. The flow rate of effluent gas from the reactor was determined using a bubble meter. The CO₂ absorption rate was then determined from the difference between the flow rates of the influent and the effluent gas. Each experiment was repeated three times.

The molar flux of CO₂ into each solution j (N_j kmol/(m²·sec)) was determined from the initial absorption rate, $V(t_1)/t_1$ using the following equation:

$$N_j = \frac{P_T - P_w^0}{SRT} \frac{V(t_1)}{t_1} \quad (1)$$

where, P_T (kPa) is the atmospheric pressure, P_w^0 (kPa) is the vapor pressure, S (cm²) is the gas-liquid contact area, R ((L·atm)/(mol·K)) is the gas constant, and T (K) is the temperature.

Another experimental system was constructed to test the amount of CO₂ absorption into each solution at equilibrium as shown in Fig. 2. A reactor with a height of 160 mm was located in a temperature-controlled vessel. Four baffles with 5 mm width were installed inside the reactor. A two-blade impeller (70 mm \times 20 mm) was also installed in the middle of the liquid level. The temperature inside the reactor was measured with a K-type thermocouple with an accuracy of ± 0.1 K. The stirring speed was limited at no more than 50 r/min to keep the gas-liquid interface

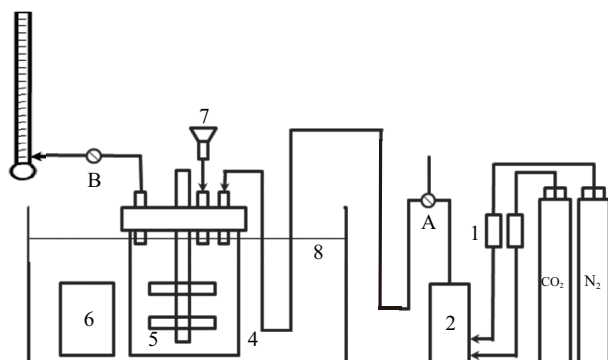


Fig. 1 Schematic diagram of the agitated vessel. (1) mass flow controller; (2) mixing chamber; (3) soap bubble meter; (4) reactor; (5) impeller; (6) liquid bottle; (7) funnel; (8) water bath.

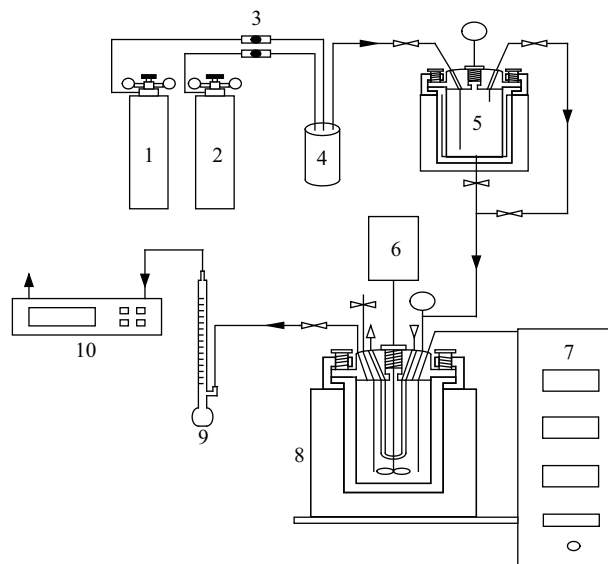


Fig. 2 Schematic diagram of experimental system used to determine CO₂ adsorption capacity. (1) N₂ cylinder; (2) CO₂ cylinder; (3) mass flow controller; (4) mixing chamber; (5) saturator; (6) magnetic drive; (7) controller of temperature and rpm; (8) reactor in a vessel; (9) soap bubble meter; (10) analyzer.

planar and smooth. Each solution of 300 mL was located in the reactor, and its absorption capacity was determined with a CO₂ partial pressure in the range of 0–600 kPa at 313 and 383 K, respectively. The CO₂ partial pressure in the reactor was recorded using a pressure data logging system (PR2000, Madgetech, USA). The CO₂ loading of each solution was calculated according to the following Eqs. (2)–(4):

$$n_{\text{object gas}} = [(P_{N_2 + \text{object gas}} - P_{\text{eq}})V]/RT \quad (2)$$

$$P_{\text{object gas}} = (P_{\text{eq}} - P_{N_2}) \quad (3)$$

$$\alpha = n_{\text{object gas}}/\text{mole of amine} \quad (4)$$

where, $n_{\text{object gas}}$ is the amount of object gas, $P_{\text{object gas}}$ is the partial pressure of object gas, P_{eq} is the equilibrium pressure, P_{N_2} is initial pressure and α is the CO₂ loading ratio.

2 Results and discussion

2.1 Solubility

CO₂ is physically soluble in an aqueous alkanolamine solution without chemical reaction. The physical solubility of CO₂ was determined from the solubility of N₂O in each solution because CO₂ reacts with the amine solution. Each KIER-C3 solution with different concentrations of 0.05, 0.10, 0.15 and 0.20 kmol/m³ was added into a 2 kmol/m³ AMP solution. Henry's constant (H) for N₂O on each AMP solution with an addition of KIER-C3 was determined at various temperatures of 293, 303, 313 and 323 K and then converted to the constant for CO₂ in the solution using Eq. (5).

$$(H_{\text{CO}_2})_{\text{amine}} = (H_{\text{N}_2\text{O}})_{\text{amine}} \times (H_{\text{CO}_2}/H_{\text{N}_2\text{O}})_{\text{water}} \quad (5)$$

As shown in Fig. 3, Henry's constant decreased with

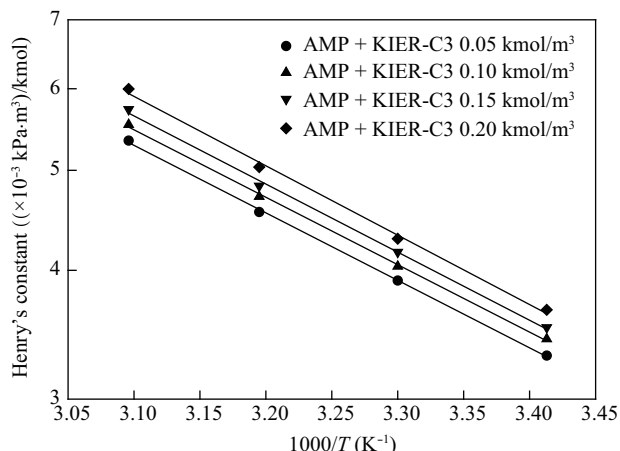


Fig. 3 Henry's constants for CO₂ in AMP/KIER-C3 solution with different KIER-C3 contents as a function of temperature.

increasing temperature and the concentration of KIER-C3 in the AMP/KIER-C3 solution. Therefore, the solubility of CO₂ in the AMP/KIER-C3 solution was found to increase with an increase in the concentration of KIER-C3.

2.2 Diffusivity

Diffusivity (D_A) of CO₂ in the AMP/KIER-C3 solution was also obtained from determining diffusivity of N₂O in the solution at the temperatures of 293, 303, 313 and 323 K by using Eq. (6).

$$(D_{\text{CO}_2})_{\text{amine}} = (D_{\text{N}_2\text{O}})_{\text{amine}} \times (D_{\text{CO}_2}/D_{\text{N}_2\text{O}})_{\text{water}} \quad (6)$$

Detailed information on the wetted wall column used to determine the diffusivity is found in our previous publication (Choi et al., 2009). As shown in Fig. 4, diffusivity of CO₂ in the AMP/KIER-C3 solution decreased with increasing KIER-C3 content for all tested temperatures. This may be attributed to the increase in the viscosity of the solution with increasing KIER-C3 content.

2.3 Absorption rate

The CO₂ absorption rate was determined for AMP, MEA, NH₃ and KIER-C3 with various concentrations of 0.5, 1.0, 1.5 and 2.0 kmol/m³ at the temperature of 313 K and

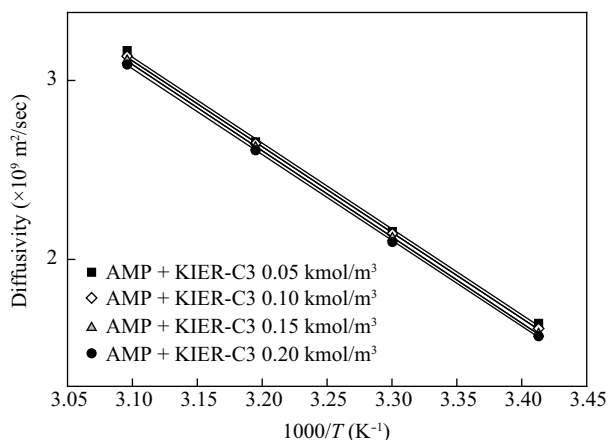


Fig. 4 Diffusivity of CO₂ in AMP/KIER-C3 solutions with different KIER-C3 contents at 2 kmol/m³ AMP as a function of temperature.

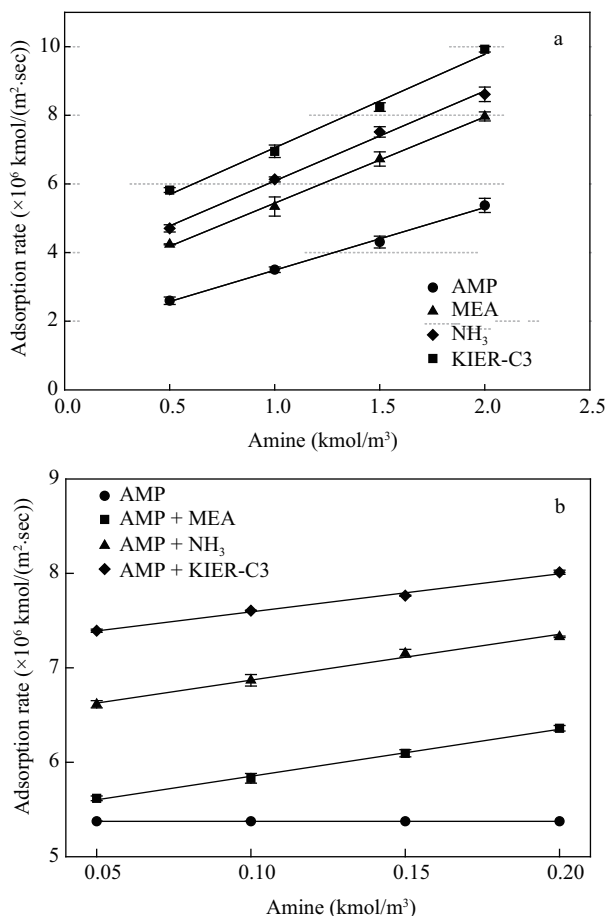


Fig. 5 Absorption rates of the CO₂ into (a) aqueous AMP, MEA, NH₃ and KIER-C3 and (b) AMP/amine solutions as a function of the concentration of each amine solution at 313 K.

the CO₂ partial pressure of 15 kPa. Figure 5a shows the absorption rate as a function of the concentration of each solution. The absorption rate increased with increasing concentration of each solution. This is caused by enhanced mass transfer in the gas-liquid interfacial area with increasing concentration. The absorption rate of CO₂ into 2 kmol/m³ KIER-C3 solution was found to be 84.7%, 24.6% and 15.2% higher than that into 2 kmol/m³ AMP, MEA and NH₃, respectively. As hydrolysis of carbamate, which is created via reaction of KIER-C3 and CO₂, is accelerated, and CO₂ within carbamate is converted to bicarbonate, the concentration of carbamate gets lower. However, since concentration of the reactant amine increases, those will be involved in absorption reaction of CO₂, and stimulates absorption to adjust lower concentration of carbamate and higher amine to equilibrium concentration, which leads to a higher reaction rate.

Figure 5b shows the CO₂ absorption rates of 2 kmol/m³ AMP with different concentrations of additives at 313 K. The absorption rates were found in the range of 5.62×10^{-6} to 8.01×10^{-6} kmol/(m²·sec). The absorption rate of the solution with an addition of KIER-C3 was 9.3%–31.6% higher than the absorption rates of other solutions with MEA and NH₃. Therefore, KIER-C3 showed the highest absorption rate for CO₂ and the best performance as an additive into AMP out of the absorbents tested in this study.

2.4 Effect of the KIER-C3 concentration on CO₂ absorption

The adsorption of CO₂ in AMP solution with an addition of KIER-C3 was tested at different temperatures. In addition to the total absorption rate of the AMP/KIER-C3 solution, the absorption rates of the AMP portion and the KIER-C3 portion in the AMP/KIER-C3 solution were determined respectively as presented in Fig. 6.

It was observed from Fig. 6 that the absorption rates into the KIER-C3 portion ($N_{\text{KIER-C3}}$) increased from 1.28×10^{-6} to 4.12×10^{-6} kmol/(m²·sec) and 1.96×10^{-6} to 6.52×10^{-6} kmol/(m²·sec) with increasing KIER-C3 concentration at the temperature of 293 and 323 K, respectively. But the absorption rate into the AMP portion (N_{AMP}) decreased with increasing KIER-C3 concentration. As a result, $N_{\text{KIER-C3}}$ was as much as 55.7% of the total absorption rate (N_{total}) at the KIER-C3 concentration of 0.2 kmol/m³.

2.5 Reaction kinetics

Reaction rate constants (k_2) for the absorption of CO₂ into AMP and AMP/KIER-C3 were determined by plotting overall reaction rate constant (k_{ov} , m³/(kmol·sec)) with the absorbent concentration at 293, 303, 313 and 323 K. By using Eq. (7), k_{ov} can be calculated as follows:

$$k_{\text{ov}} = k_{\text{m}} = (N_A H_A^{(m+1)/2} / P_A^{(m+1)/2} / D_A^{1/2})^2 \quad (7)$$

where, N_A (m³/(kmol·sec)) is the overall absorption rate, H_A ((kPa·m³)/kmol) is the Henry's constant, P_A (kPa) is the partial pressure, D_A (m²/sec) is the diffusivity of CO₂, m is the order of reaction with respect to species A, and n is the order of reaction with respect to CO₂.

The reaction of CO₂ with the AMP/KIER-C3 solution can be classified as a fast pseudo first-order reaction. We confirmed the reaction order by plotting Eq. (7) with the concentration of KIER-C3 in the solution. Figure 7 shows straight lines with a slope of 1. In addition, the k_{ov} value increased linearly with increasing the temperature and the concentration of KIER-C3 in the solution. This may be

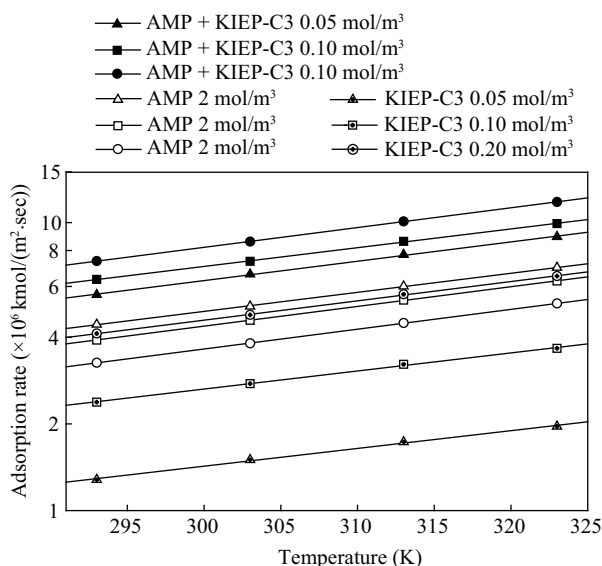


Fig. 6 Absorption rate of CO₂ into the AMP/KIER-C3 solution at different temperatures.

attributed to the increased diffusion at the gas-liquid interface with increasing the temperature and concentration.

The reaction rate constants (k_2) were then determined for the absorption of CO₂ into AMP and AMP/KIER-C3 at different temperatures and shown in Table 1. The values of k_2 were found to be 530.98–1323.81 m³/(kmol·sec) for AMP and 3939.53–7347.65 m³/(kmol·sec) for AMP/KIER-C3. Hence the k_2 values for a blend of AMP and KIER-C3 were five to six times higher than that for AMP without KIER-C3. This result shows that the reactivity of AMP is significantly enhanced with an addition of KIER-C3. Therefore, KIER-C3 is considered to be an effective activator in the AMP solution. This may be attributed that KIER-C3 has two amine groups which have characteristic of sterically hindered amine. While primary amine forms stable carbamate, sterically hindered amine forms more instable carbamate. The reduction in stability promotes hydrolysis of carbamate and CO₂ absorption. Because KIER-C3 has two sterically hindered amine groups, KIER-C3 may act as an effective activator in the AMP solution.

Figure 8 shows the correlation between reaction rate constant (k_2) and temperature using the results in Table 1. From a linear regression analysis ($r^2 = 0.99$), the following equations were obtained for the relationship between k_2 and temperature.

$$k_{2,\text{AMP}} = 1.079 \times 10^7 \exp(-2909.16/T) \quad (8)$$

$$k_{2,\text{AMP/C3}} = 7.702 \times 10^6 \exp(-2248.03/T) \quad (9)$$

From the exponents in the Arrhenius equations, activation energies for the reaction of CO₂ with AMP and

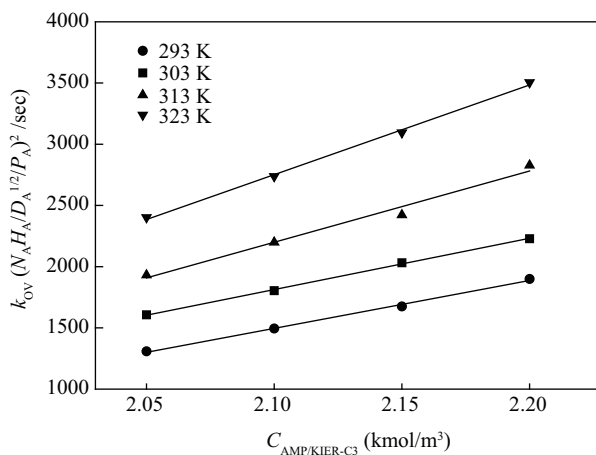


Fig. 7 Pseudo first-order overall reaction rate constant for the reaction of CO₂ with AMP/KIER-C3 solution at different temperatures.

Table 1 The second-order reaction rate constant calculated for the reaction of CO₂ into aqueous AMP and 2 kmol/m³ AMP/KIER-C3 solutions as a function of temperature

Temperature (K)	AMP (m ³ /(kmol·sec))	AMP + KIER-C3 (m ³ /(kmol·sec))
293	530.98	3939.53
303	730.53	4146.09
313	992.78	5976.13
323	1323.81	7347.65

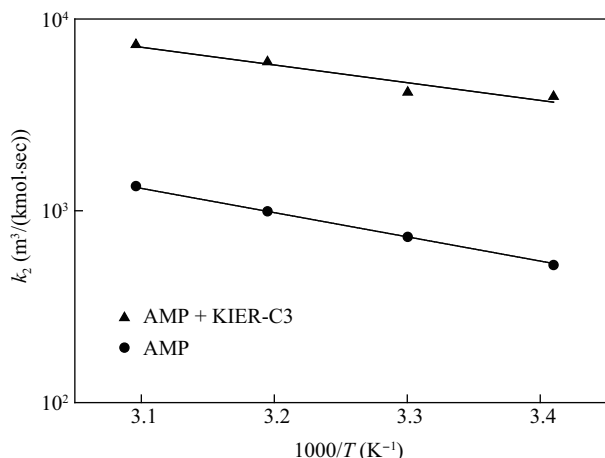
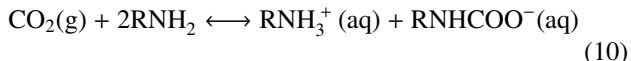


Fig. 8 Arrhenius plot for the correlation between reaction rate constant and temperature.

AMP/KIER-C3 were determined to be 24.2 and 18.7 kJ/mol, respectively. The lower activation energy for AMP/KIER-C3 also indicates that the reactivity of AMP for CO₂ is enhanced with an addition of KIER-C3.

2.6 Absorption equilibrium

The reaction of CO₂ with the primary amino group can produce three possible reactions: the formation of carbamate and bicarbonate, the reversion of carbamate to bicarbonate, or the formation of the carbonate ion (Yih et al., 1988).



The equilibrium loading capacities of primary and secondary amines are limited by stoichiometry (0.5 mol of CO₂/mol of amine) of Eq. (10). The zwitterions mechanism originally proposed by Caplow (1968) and reintroduced by Danckwerts (1979) is generally accepted

as the reaction mechanism for Eq. (10) (Blauwhoff et al., 1983).



where, B' is amine, OH⁻ or H₂O. The carbamates formed from primary and secondary amines are quite stable. If the carbamate ion is unstable, as in the case of a hindered amine, it undergoes the formation of bicarbonate ion as in Eq. (11). This reaction means that 1 mol of hindered amine allows loading of CO₂ up to 1 mol.

The CO₂ loading ratio is the most basic factor to evaluate the performance of absorbents. CO₂ loading in each 2 kmol/m³ solutions of AMP, MEA, NH₃ and KIER-C3 was determined respectively with increasing CO₂ partial pressure at 313 K. The highest CO₂ loading in the AMP, MEA, NH₃ and KIER-C3 solution was 0.72, 0.82, 0.93 and 2.88 mol CO₂/mol absorbent, respectively, in the range of CO₂ partial pressure as shown in Fig. 9a. Hence KIER-C3 was found to have three to four times higher CO₂ loading than other solutions. The higher CO₂ loading in KIER-C3 may be attributed that KIER-C3 has two nitrogen compounds which have characteristics of sterically hindered amine. In addition, the CO₂ loading of more than 2 mol CO₂/mol absorbent indicates that intermediate products formed during the reaction act as the absorbents for CO₂.

In the full-scale CO₂ separation process using alkanolamine solutions, CO₂ absorption and stripping systems may be operated at the temperature range of 310–320 K and 380–400 K, respectively. To examine CO₂ loadings in blended amines at the absorption and stripping temperatures, each AMP solution with different additives was tested at 313 and 383 K. As shown in Fig. 9b, AMP/KIER-C3 shows much higher CO₂ loading at 313 K and similar CO₂ loading as the other absorbents at 383 K. Hence, AMP/KIER-C3 shows 2 and 3.4-times higher difference in CO₂ loading compared to AMP/NH₃ and AMP/MEA,

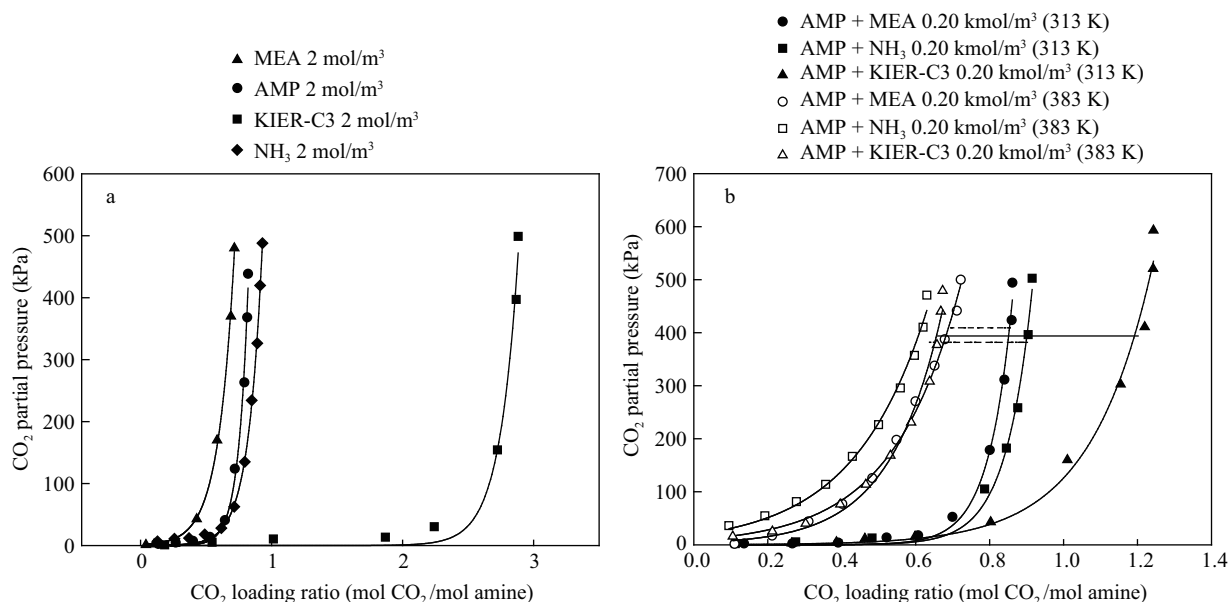


Fig. 9 CO₂ loading in AMP, MEA, NH₃ and KIER-C3 with increasing CO₂ partial pressure at 313 K (a) and in AMP with different additives at 313 and 383 K and AMP 2 kmol/m³ (b).

respectively. This suggests that KIER-C3 can be used as an excellent additive to AMP in the CO₂ separation process.

3 Conclusions

Absorption of CO₂ into AMP/KIER-C3 was tested using a stirred batch tank reactor with different concentrations and reaction temperatures. The absorption rate into the aqueous KIER-C3 solution were 84.7%, 24.6% and 15.2% higher than that into aqueous AMP, MEA and NH₃ solution at 313 K, respectively. Also, the CO₂ absorption rate on the addition of KIER-C3 into 2 kmol/m³ AMP solutions increased by 9.3% to 31.6% compared to the addition of MEA and NH₃ solution, respectively. This may be ascribed to the increase in diffusion and contact between the CO₂ and KIER-C3. KIER-C3 showed the best performance as an additive to increase CO₂ absorption rate of AMP. The calculated reaction rate constant for the reaction of CO₂ into aqueous AMP and AMP/KIER-C3 solution was determined to be $k_{2,AMP} = 1.079 \times 10^7 \exp(-2909.16/T)$ and $k_{2,AMP/C3} = 7.702 \times 10^6 \exp(-2248.03/T)$, respectively. In addition, activation energies of AMP and AMP/KIER-C3 were found to be 24.16 and 18.62 kJ/mol, respectively. The reactivity of AMP was enhanced with an addition of KIER-C3. CO₂ loading in a KIER-C3 solution was three to four times higher than other solutions such as AMP, MEA and NH₃. Also, CO₂ loading in the AMP/KIER-C3 solution was 2 and 3.4-times higher than that of the AMP/NH₃ solution and the AMP/MEA solution, respectively. Therefore, KIER-C3 may be used as an excellent absorbent or additive to AMP for the separation of CO₂ from flue gases.

Acknowledgments

This research was financially supported by the Brain Korea 21 Project in 2012 and by the Energy Efficiency & Resources of the Korea Institute of Energy Technology Evaluation and Planning (KETEP) grant funded by the Korea government Ministry of Knowledge Economy (No. 2006CCD11P011A -21-3-010).

References

- Aroonwilas A, Veawab A, 2004. Characterization and comparison of the CO₂ absorption performance into single and blended alkanolamines in a packed column. *Industrial & Engineering Chemistry Research*, 43(9): 2228–2237.
- Blauwhoff P M M, Versteeg G F, van Swaaij W P M, 1983. A study on the reaction between CO₂ and alkanolamines in aqueous solutions. *Chemical Engineering Science*, 38(9): 1411–1429.
- Caplow M, 1968. Kinetics of carbamate formation and breakdown. *Journal of the American Chemical Society*, 90(24): 6795–6803.
- Choi W J, Min B M, Seo J B, Park S W, Oh K J, 2009. Effect of ammonia on the absorption kinetics of carbon dioxide into aqueous 2-amino-2-methyl-1-propanol solutions. *Industrial & Engineering Chemistry Research*, 48(8): 4022–4029.
- Dawodu O F, Meisen A, 1994. Degradation of alkanolamine blends by carbon dioxide. *The Canadian Journal of Chemical Engineering*, 74(6): 960–966.
- Danckwerts P V, 1979. The reaction of CO₂ with ethanolamines. *Chemical Engineering Science*, 34(4): 443–446.
- Gadalla M A, Olujic Z, Jansens P J, Jobson M, Smith R, 2005. Reducing CO₂ emissions and energy consumption of heat-integrated distillation systems. *Environmental Science & Technology*, 39(17): 6860–6870.
- Hong S Y, Li M H, 2002. Kinetics of absorption of carbon dioxide into aqueous solutions of monoethanolamine + triethanolamine. *Industrial & Engineering Chemistry Research*, 41(2): 257–266.
- Lee D H, Choi W J, Moon S J, Ha S H, Kim I G, Oh K J, 2008. Characteristics of absorption and regeneration of carbon dioxide in aqueous 2-amino-2-methyl-1-propanol / ammonia solutions. *Korean Journal of Chemical Engineering*, 25(2): 279–284.
- Li M H, Chang B C, 1994. Solubilities of carbon dioxide in water + monoethanolamine + 2-amino-2-methyl-1-propanol. *Journal of Chemical & Engineering Data*, 39(3): 448–452.
- Sartori G, Savage D W, 1983. Sterically hindered amines for CO₂ removal from gases. *Industrial & Engineering Chemistry Fundamentals*, 22: 239.
- Xu S, Wang Y W, Otto F D, Mather A E, 1991. Rate of absorption of carbon dioxide in a mixed solvent. *Industrial & Engineering Chemistry Research*, 30(9): 1213–1217.

JOURNAL OF ENVIRONMENTAL SCIENCES

Editors-in-chief

Hongxiao Tang

Associate Editors-in-chief

Nigel Bell Jiuhui Qu Shu Tao Po-Keung Wong Yahui Zhuang

Editorial board

R. M. Atlas University of Louisville USA	Alan Baker The University of Melbourne Australia	Nigel Bell Imperial College London United Kingdom	Tongbin Chen Chinese Academy of Sciences China
Maohong Fan University of Wyoming Wyoming, USA	Jingyun Fang Peking University China	Lam Kin-Che The Chinese University of Hong Kong, China	Pinjing He Tongji University China
Chihpin Huang "National" Chiao Tung University Taiwan, China	Jan Japenga Alterra Green World Research The Netherlands	David Jenkins University of California Berkeley USA	Guibin Jiang Chinese Academy of Sciences China
K. W. Kim Gwangju Institute of Science and Technology, Korea	Clark C. K. Liu University of Hawaii USA	Anton Moser Technical University Graz Austria	Alex L. Murray University of York Canada
Yi Qian Tsinghua University China	Jiuhui Qu Chinese Academy of Sciences China	Sheikh Raisuddin Hamdard University India	Ian Singleton University of Newcastle upon Tyne United Kingdom
Hongxiao Tang Chinese Academy of Sciences China	Shu Tao Peking University China	Yasutake Teraoka Kyushu University Japan	Chunxia Wang Chinese Academy of Sciences China
Rusong Wang Chinese Academy of Sciences China	Xuejun Wang Peking University China	Brian A. Whitton University of Durham United Kingdom	Po-Keung Wong The Chinese University of Hong Kong, China
Min Yang Chinese Academy of Sciences China	Zhifeng Yang Beijing Normal University China	Hanqing Yu University of Science and Technology of China	Zhongtang Yu Ohio State University USA
Yongping Zeng Chinese Academy of Sciences China	Qixing Zhou Chinese Academy of Sciences China	Lizhong Zhu Zhejiang University China	Yahui Zhuang Chinese Academy of Sciences China

Editorial office

Qingcai Feng (Executive Editor) Zixuan Wang (Editor) Suqin Liu (Editor) Zhengang Mao (Editor)
Christine J Watts (English Editor)

Journal of Environmental Sciences (Established in 1989)

Vol. 24 No. 5 2012

Supervised by	Chinese Academy of Sciences	Published by	Science Press, Beijing, China
Sponsored by	Research Center for Eco-Environmental Sciences, Chinese Academy of Sciences		Elsevier Limited, The Netherlands
Edited by	Editorial Office of Journal of Environmental Sciences (JES) P. O. Box 2871, Beijing 100085, China Tel: 86-10-62920553; http://www.jesc.ac.cn E-mail: jesc@263.net , jesc@rcees.ac.cn	Distributed by	Domestic Science Press, 16 Donghuangchenggen North Street, Beijing 100717, China Local Post Offices through China Foreign Elsevier Limited http://www.elsevier.com/locate/jes
Editor-in-chief	Hongxiao Tang	Printed by	Beijing Beilin Printing House, 100083, China
CN 11-2629/X	Domestic postcode: 2-580	Domestic price per issue	RMB ¥ 110.00

ISSN 1001-0742



jesc.ac.cn